pointed out. The observed behavior for aluminum impurity is the same as that for boron. It is interesting that, in contrast to the results for $\mathbf{F}\|\langle 111\rangle$, the dependence of Δu on Δg appears to be linear.

V. CONCLUSIONS

In conclusion, the present zero-stress measurements have revealed a wealth of detail not previously observed. Also, comparison of the various experimentally observed features with the existing effective-mass calculations points to a definite need for a renewed theoretical investigation of this problem. In particular, such a theory should be able to account for the chemical species dependence of the excited states. As pointed out in Sec. IVA, the excited states of the various impurities do show a correspondence in spite of these species dependent features. The piezospectroscopic effects support this conclusion as far as the gross features are concerned. The symmetry of the ground state of all the impurities has been established to be Γ_8 of $\bar{T}_d$, in agreement with Schechter's theory.[46,47] It has been deduced that the final states of lines 1, 2, 3, and 5 of boron also belong to Γ_8. The excited state of line 4 of boron behaves in a manner consistent with an assignment of $\Gamma_6+\Gamma_7$, while that of line 4A is consistent with its being a Γ_8 state. For the impurities aluminum, gallium, and indium the symmetries of all these states agree with those of the corresponding states of boron in all the cases where unambiguous results were observed. It has been possible to obtain some insight into the gross features of the relative intensities of the stress-induced components of a given line on the basis of the symmetries of the states participating in the transition. Quantitative differences have been observed in the stress behavior of the corresponding states of the various impurities as well as between states of a given impurity.

ACKNOWLEDGMENTS

The authors wish to thank Professor H. J. Yearian and Miss Louise Roth for orienting the samples used in the present investigation. They are also indebted to S. Balasubramanian for writing a major subroutine that was used in the data analysis.

PHYSICAL REVIEW VOLUME 163, NUMBER 3 15 NOVEMBER 1967

Photoelectric Emission from InAs: Surface Properties and Interband Transitions

T. E. FISCHER,* F. G. ALLEN,† AND G. W. GOBELI‡
Bell Telephone Laboratories, Murray Hill, New Jersey
(Received 13 June 1967)

Photoelectric yield spectra and energy distributions at photon energies between 2.8 and 6.2 eV have been measured for the (110) surface of InAs cleaved in high vacuum and covered with various amounts of cesium. Cleavage produces an inversion layer on the n-type crystal investigated ($N_D=2.5\times10^{15}$ cm^{-3}); on a clean surface the Fermi level coincides with the top of the valence band. The electron affinity and work function of the clean (110) surface are $\chi=4.55\pm0.05$ eV and $\varphi=4.90\pm0.05$ eV, respectively. Deposition of 1/20 monolayer of cesium results in a degenerate n-type surface, which indicates a low density of surface states in the energy gap. Our measurements confirm several important interband transitions in InAs, namely, the Γ_{15v}-Γ_{15c} transition at $h\nu=4.30$ eV, an L_{3v}-L_{3c} transition near $h\nu=6$ eV with a new position of L_{3v} at 1.3 and 1.6 eV below Γ_{15v}, and an X_{5v}-X_{1c} transition at 4.50 eV. We also report two transitions not observed previously. Whatever information can be gained about conservation of the $\mathbf{k}$ vector points to a strong predominance of direct transitions.

I. INTRODUCTION

PHOTOELECTRIC emission has been used for the investigation of surfaces and more extensively for the determination of optical properties and the energy-band structures of solids. In such experiments, one measures the photoelectric yield Y, or total number of electrons emitted per absorbed photon, and the energy distributions dY/dE of the emitted electrons as a function of the photon energy $h\nu$. In surface studies, the interest is concentrated on the determination and interpretation of the photoelectric threshold and the emission properties of neighboring photon energies.[1–8] For the determination of optical properties, on the other hand, one progressively lowers the work function of the

* Present address: Yale University, New Haven, Connecticut.
† Present address: Bellcomm Inc., Washington, D. C.
‡ Present address: Sandia Corporation, Albuquerque, New Mexico.

[1] E. O. Kane, Phys. Rev. **127**, 131 (1962).
[2] G. W. Gobeli and F. G. Allen, Phys. Rev. **127**, 141 (1962).
[3] F. G. Allen and G. W. Gobeli, Phys. Rev. **127**, 150 (1962).
[4] J. J. Scheer and J. van Laar, Phys. Letters **3**, 246 (1963).
[5] G. W. Gobeli and F. G. Allen, Surface Sci. **2**, 402 (1964).
[6] F. F. Scheer and J. van Laar, Surface Sci. **3**, 189 (1965).
[7] G. W. Gobeli and F. G. Allen, Phys. Rev. **137**, A245 (1965).
[8] T. E. Fischer, Phys. Rev. **142**, 519 (1966).

emitter by depositing fractions of a monolayer of a substance (usually cesium) and observes the emergence of electrons excited to energy levels sufficiently high for escape.[8–13] Further insight into the final states of optical transitions can be gained from the measurement of energy distributions.

Strong correlations are generally obtained between the photoelectric-yield spectrum $Y(h\nu)$ and other optical properties and the yield itself agrees fairly well with theoretical predictions.[9,14,15] Cohen and Phillips[13] have offered an interpretation of yield spectra of several III–V compounds[16] in terms of critical points in the joint density of states; they correlated structure in the yield curves with interband splittings in the computed energy bands at points of high symmetry in the Brillouin zone (Γ,X,L). Similar agreement has been found previously between yield spectra and band structures in the case of silicon.[12]

The interpretation of the energy distributions of emitted electrons presents serious difficulties. In the case of silicon, the energy distributions computed on the basis of the band structure and optical transitions alone[15] do not agree with experimental results.[12] The general behavior of the energy distributions has prompted Spicer to conclude that in many metals and semiconductors, conservation of the **k** vector of the electrons during optical transitions is not an important selection rule,[17] a result which contradicted previous assumptions. Following a different line of thought, Kane[18] improved the interpretation of energy distributions by accounting for the effects of energy losses and group velocities of the excited electrons on their way towards the surface. These effects were found to exert a considerable influence on the shape of the energy distribution curves.

In the present work, we present the results of photoelectric emission measurements, including spectral dependence of the total yield and the energy distributions from two InAs crystals that were cleaved in ultrahigh vacuum and covered with various amounts of cesium. Since Cohen and Phillips[13] have presented and interpreted our yield spectra in an earlier paper, the present work will emphasize the measurement and interpretation of the energy distributions. The yield curves are shown again because they contain certain information pertaining to surface properties not discussed by Cohen and Phillips, and also because a discussion of the energy distributions is not practical without reference to the yield spectrum.

II. EXPERIMENTAL TECHNIQUES

The experimental techniques, their possibilities and limitations have been described in detail previously,[12] so that we only summarize them briefly. The experimental arrangement consists of a Pyrex vacuum tube with a quartz window through which uv radiation from a Bausch and Lomb 500 mm grating monochromator equipped with a mercury arc or hydrogen discharge source is admitted. The sample surface is prepared by cleavage in a vacuum of 10^{-10} Torr and subsequent coverage with the desired amount of cesium. For the determination of the total yield, one measures the current from the sample while all other components of the tube are maintained at collecting potential; this eliminates the danger of measuring electrons emitted from other electrodes by scattered light. Total energy distributions are measured with the retarding-field method. The electron-retarding electrode consists of a cylindrical mesh enclosure covered with an evaporated film of gold. The retarding voltage changes linearly with time so that the energy distributions dY/dE can be obtained by electronic differentiation. The energy resolution is estimated from the half-width of the narrowest distribution; it is better than 0.15 eV. However, fringe fields between the cesium-covered surface and the oxydized side faces of the sample cause distortions at the low-energy end of the distributions at low-work functions. For a discussion of these limitations see Ref. 12. Work functions are determined by the Kelvin method, e.g., by vibrating a molybdenum probe in front of the surface and adjusting the voltage between the two so as to obtain zero ac current flowing. This voltage, known as the contact potential difference (CPD), is then the difference in work functions of the two surfaces. The work function of the Mo probe is determined by measuring the CPD with a clean tungsten ribbon whose work function is determined by photoemission. Work-function determinations are believed accurate to ± 0.05 eV. The two samples investigated were cut from the same crystal with the following characteristics at room temperature: $\rho = 0.01\ \Omega$ cm, N-type, $\mu = 26\,500$ cm^2 V^{-1} sec^{-1}. For such doping, the Fermi level lies approximately 0.025 eV below the bottom of the conduction band in the bulk. The energy gap of InAs at room temperature is 0.35 eV. Integration of the Poisson equation shows that if the surface is degenerate n type (which we will see in Sec. IV to be the case once we deposit 0.05 monolayer of cesium or more), the bands can be considered flat within 0.04 eV for all distances greater than 15 Å away from the surface.

[9] W. E. Spicer and R. E. Simon, Phys. Rev. Letters **9**, 385 (1962).

[10] W. E. Spicer and R. E. Simon, J. Phys. Chem. Solids **23**, 1817 (1962).

[11] T. E. Fischer, Phys. Rev. **139**, A1228 (1965).

[12] F. G. Allen and G. W. Gobeli, Phys. Rev. **144**, 558 (1966).

[13] M. L. Cohen and J. C. Phillips, Phys. Rev. **139**, A912 (1965).

[14] D. Brust, M. L. Cohen and J. C. Phillips, Phys. Rev. Letters **9**, 389 (1962).

[15] D. Brust, Phys. Rev. **139**, A489 (1965).

[16] F. G. Allen and G. W. Gobeli (unpublished).

[17] C. N. Berglund and W. E. Spicer, Phys. Rev. **136**, A1044 (1964); N. B. Kindig and W. E. Spicer, *ibid.* **138**, A561 (1965); W. E. Spicer and G. J. Lapeyre, *ibid.* **139**, A565 (1965).

[18] E. O. Kane, Phys. Rev. **147**, 335 (1966); E. O. Kane, in *Proceedings of the International Conference on the Physics of Semiconductors* [J. Phys. Soc. Japan, Suppl. **21**, 37 (1966)].

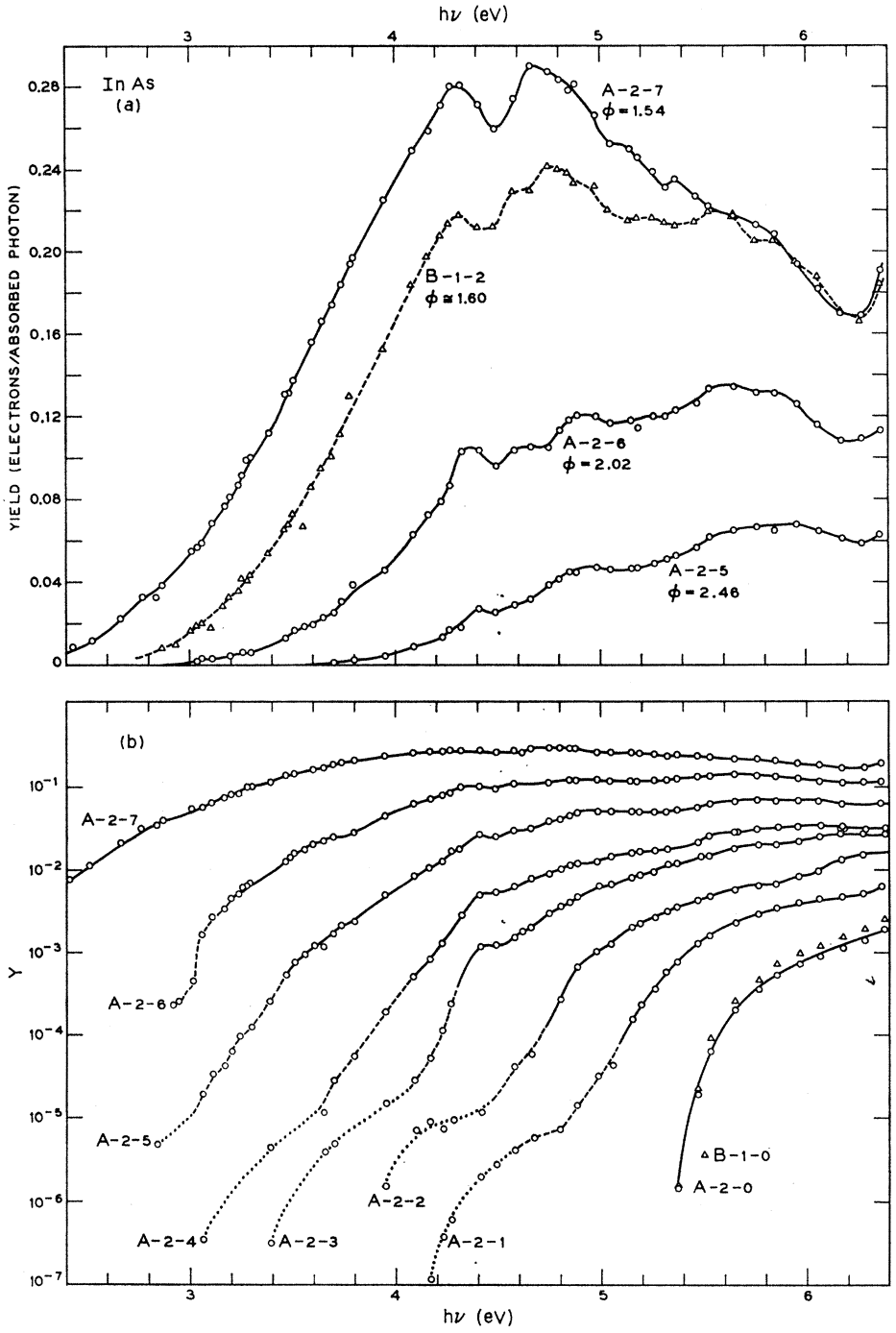

FIG. 1. Photoelectric-yield spectra of InAs. φ=work functions in eV. (a) Linear plot; (b) semilogarithmic plot. The dotted lines correspond to electrons originating from the conduction band, the solid lines to emission out of the valence band, the dashed line to both simultaneously (see text).

The photoelectric yield Y shown in Fig. 1 is the number of electrons emitted per absorbed photon. The light intensity falling on the sample was measured with a calibrated detector; allowance was made for the reflected light by using the reflectivity values of Phillip and Ehrenreich.[19] The energy distributions (Figs. 2–5) are normalized, i.e., the area under each curve is equal to the yield Y at the corresponding photon energy. The abscissa of Figs. 2(a), 4, 5(a) gives the energy E of the emitted electrons with respect to the top of the valence band E_v in the bulk. In Figs. 2(b) and 5(b), the same energy distributions are shown in a way which emphasizes the initial states of the transitions, rather than the final or emission energies. To this end we subtract the photon energy $h\nu$ from the final energy E by displacing the distributions of Figs. 2(a) and 5(a) to the left on

[19] H. R. Philipp and H. Ehrenreich, Phys. Rev. **129**, 1550 (1963).

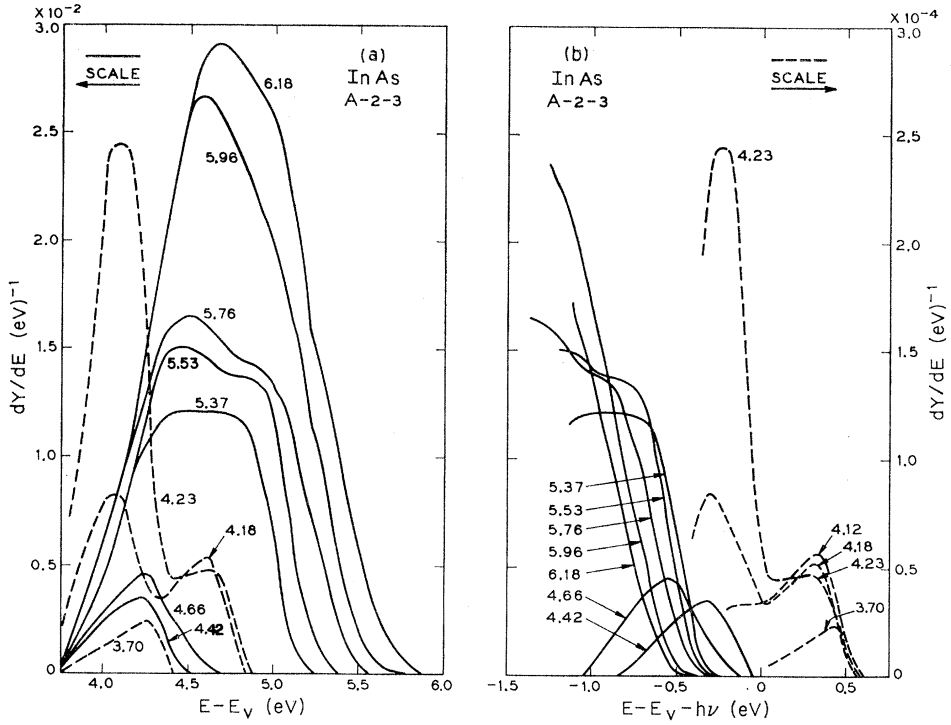

FIG. 2. Energy distributions of photoelectrons from InAs corresponding to the yield curve *A*-2-3. (a) The abscissa measures the energy of the emitted electrons relative to the top of the valence band E_v in the bulk. In plot *b* the same distributions were displaced by $h\nu$, the abscissa then shows the initial energies of the electrons with respect to E_v. The left-hand scale pertains to the solid curves, the right-hand scale to the dashed curves which are magnified 100× with respect to the others. The numbers are the photon energies in eV.

the abscissa by the amount $h\nu$. In Fig. 3, we plot the energy of the electrons with respect to the Fermi level: $E-E_F$.

The energy values $E-E_v$ and $E-E_F$ represented in the abscissas of Figs. 2–5 are not an immediate experimental result. In practice one applies a known potential difference V between the emitter and the collector and measures the current due to electrons whose energy exceeds the potential at the surface of the collector

$$E \geq E_F + V + \varphi_c, \tag{1}$$

where E_F is the Fermi level of the emitter and φ_c the work function of the collector. The latter is difficult to measure directly but can be determined from (1) if some particular electron energies are known.

One such value of E is the "saturation point"; that is the minimum energy E_m at which electrons are emitted. Clearly, $E_m-E_F=\varphi$. The work function φ of the emitter can be measured by the Kelvin method. Figure 3 illustrates this possibility: The arrows on the abscissa correspond to the work functions of the clean surface ($\varphi=4.90$ eV) and of the surface covered with 5×10^{13} cm^{-2} cesium atoms ($\varphi=4.19$ eV). The low-energy cutoffs of the energy distributions (Fig. 3) must be displaced by half the energy resolution of the analyzer. This method can only be used where the work function is homogeneous over the emitting surface and where fringe fields are negligible, i.e., with clean surfaces.

The highest energies at which electrons are emitted can also measure φ_c through (1) provided that their significance can be clearly established. We shall demonstrate in Sec. IV that the distributions drawn in dashed lines in Figs. 2 and 3 result from excitation out of the degenerate conduction band: The high-energy limit of these distributions corresponds to $E_{\max}=E_F+h\nu$. (The deparature from a vertical drop is a measure of the limited energy resolution.)

In Sec. V we discuss the emission of electrons excited from the valence band. We shall find there that the high-energy limit for the distributions obtained at $h\nu=4.41$ eV corresponds to electrons emitted from the top of the valence band. This fact allows us to circumvent Eq. (1) and calibrate the abscissa in Figs. 4 and 5 directly by setting $E-E_v=h\nu=4.41$ eV at the high-energy cutoff of the corresponding energy distribution. By considering the position of the Fermi level in the bulk ($E_F-E_v=0.325$ eV) we find for the work function of the collector a value which agrees with that determined through the saturation point and the degenerate conduction band: $\varphi_c=4.75\pm0.1$ eV.

III. CRITERIA FOR THE INTERPRETATION

We have pointed out in the introduction that the interpretation of measured energy distributions still presents a serious problem. In general, the experimental data contain less structure and vary less with photon energy than simple theory predicts. In particular, the position of peaks in the energy distributions should depend on the photon energy if the optical transitions are direct[14] (that is, if the wave vector k of the electrons is conserved). Instead, one often observes

peaks that vary in amplitude, but not in energy position over a considerable range of photon energies.[8,11,12,17]

Kane[18] has been able to improve the agreement between theoretical and experimental distributions by showing that energy losses due to scattering of the excited electrons on their way towards the surface play an important role in determining the shape of emitted energy distributions. In the case of silicon, for which the computations were made (and probably also for III–V compounds) interactions with optical phonons are the dominant energy-loss mechanism throughout the energy range covered by our experiments ($h\nu \leq 6.2$ eV). Pair creation becomes more important at higher energies. The lifetime of an electron with respect to phonon scattering is proportional to the inverse $1/\rho(E)$ of the density of electron states, and so is the average group velocity. Consequently, electrons excited to an energy where the density of states is high will suffer many more collisions (losing approximately 0.05 eV/collision) before emission than at energies with low state density. A peak in the density of states may, therefore, lead to a dip in the measured dY/dE at the same energy followed by a peak at somewhat lower energy.

In interpreting the energy distributions of Figs. 4 and 5, we will be faced with the task of determining which structure is due to the energy-dependent scattering and which to optical transitions. It is obviously impossible to make a rigorous distinction, but we will be assisted by the fact that all structure introduced during the emission process subsequent to optical excitation (by scattering or energy-dependent reflection at the surface barrier) will depend on the final energy of the electrons only. In Figs. 4 and 5, therefore, transport effects will produce the same deformation at a given value of $E-E_v$ for all energy distributions measured at various $h\nu$. On the contrary, structure which depends on the photon energy, and in particular peaks that move as $h\nu$ is changed or that appear in a limited range of photon energies only, can be attributed to optical transitions and details in the band structure.

Kane's recent analysis of the band structure and optical properties of silicon[20] commands great prudence in the assignments of structure to transitions at points of high symmetry in the Brillouin zone. In effect, he has shown that there are peaks in the joint density of states of Si, causing prominent structure in reflectivity and photoelectric-yield spectrum $Y(h\nu)$ that are not due to one strong critical point of high symmetry, but to an accumulation of less important transitions in various parts of the Brillouin zone, a fact which has been experimentally observed for GaP.[21] In most cases, then, we will have to limit ourselves to the description of the observed transitions, the approximate energy of their final and initial states and to the suggestion of compatible transitions in the energy bands. A more detailed interpretation of our results would require an analysis similar to that performed by Kane in the case of silicon.[20] For such an interpretation, it would certainly be useful to extract from our data some information about the relative importance of direct and indirect transitions.

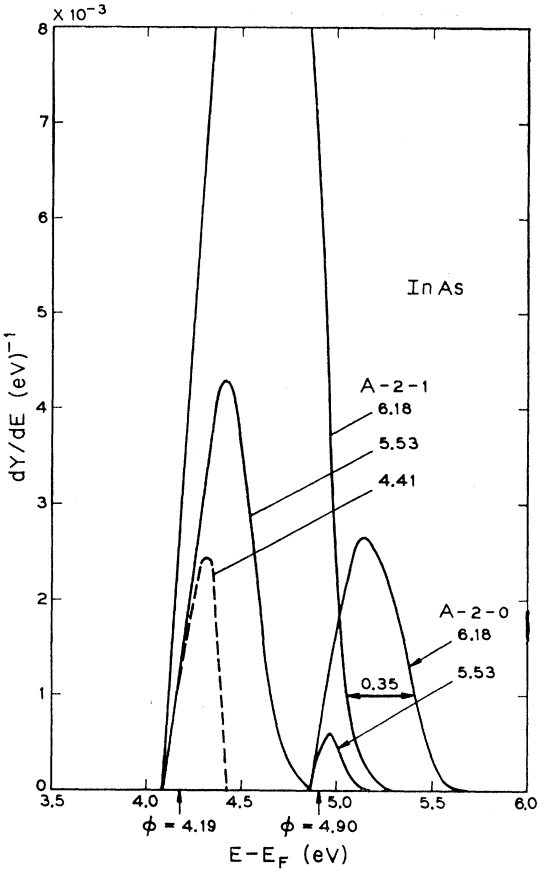

FIG. 3. Energy distributions of photoelectrons from InAs corresponding to yields A-2-0 (clean surface) and A-2-1. The abscissa shows the energies of the emitted electrons with respect to the Fermi level. The numbers are the photon energies. The distribution for $h\nu = 4.41$ eV is magnified 100× with respect to the others. It is made of electrons excited from the vicinity of the Fermi level.

Unequivocal information can be obtained from the transitions out of the top of the valence band (Γ_{15v}). These transitions are separated from all others, being the only ones with such high initial energy. Also, the electrons excited out of the top of the valence band which form the high-energy limit of distributions, are certainly not the result of scattering mechanisms. The following arguments indicate that optical transitions out of the top of the valence band of InAs *do not* obey the predictions for indirect transitions.

Suppose that the **k** vector of the electrons varies at random during excitation. Then the transition probability is proportional to the density of initial $N_v(E_i)$ and final states $N_c(E_f)$. The energy distributions are given by

$$dY/dE \simeq |M|^2 N_c(E_f) N_v(E_i) T(E_f), \qquad (2)$$

[20] E. O. Kane, Phys. Rev. **146**, 558 (1966).
[21] T. E. Fischer, Phys. Rev. **147**, 603 (1966).

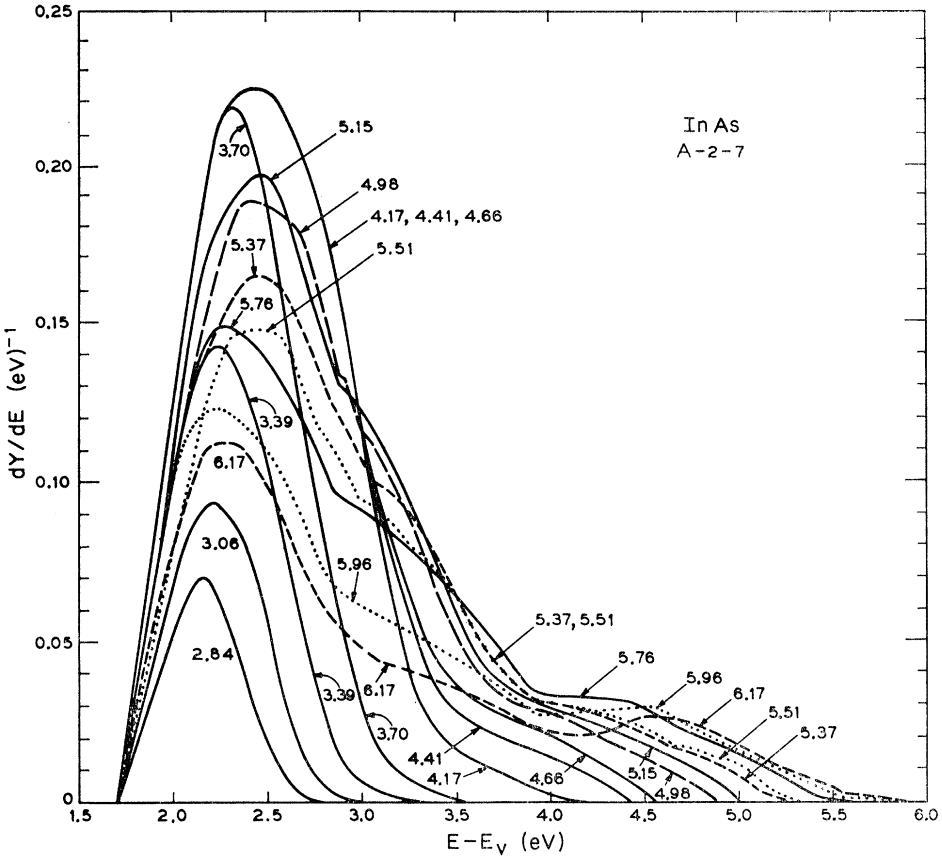

FIG. 4. Energy distributions of photoelectrons from InAs covered with a monolayer of cesium (yield *A*-2-7). The numbers are equal to the photon energies. The abscissa shows the the energy of the emitted electrons with respect to the top of the valence band.

where $|M|^2$ is the square of a matrix element and $T(E_f)$ the probability that the electron excited to the final energy E_f escape. (E_f for final states, not to be confused with E_F for Fermi level.) We set into Eq. (4) the known density of states near the top of the valence band and we obtain for a plot of energy distributions emphasizing the initial states as in Fig. 5(b) :

$$\frac{dY}{dE}(E_i)\simeq(E_v-E_i)^{1/2}C|M|^2N_c(E_i+h\nu)T(E_i+h\nu). \quad (3)$$

In other words, all energy distributions in Fig. 5(b) should have approximately the same shape $\sim(E_v-E_i)^{1/2}$ and strictly the same high-energy limit $E-E_v-h\nu=0$; only the amplitude of the high-energy end should vary proportionally to

$$|M|^2N_c(E_f)T(E_f).$$

Clearly, Fig. 5(b) is incompatible with indirect transitions: the shape of the distributions changes rapidly for $h\nu\leq 4.41$ eV and the upper ends of the distributions do not coincide in energy at higher photon energies. We shall come back to this point in Sec. V. (This argument holds true only for the high-energy end of the distributions).

IV. DISCUSSION: SURFACE PROPERTIES

In this section, we analyze the energy distributions and photoelectric-yield spectra and extract that information which pertains to the surface properties of InAs.

Let us first summarize the evidence leading to the conclusion that all cesium coverages we applied ($\theta\geq 0.05$ monolayer) resulted in a degenerate n-type surface with the Fermi level well inside the conduction band. Fig. 2 displays the energy distributions corresponding to the yield curve *A*-2-3 of Fig. 1; (cesium coverage$=2.3\times10^{14}$ cm^{-2}; $\varphi=3.4$ eV). The plot of Fig. 2(b) shows the energy of the initial states as we have discussed in Sec. II.

The solid curves represent normalized energy distributions for photon energies $h\nu\geq 4.41$ eV, as measured with the scale to the left of the figure. Energy distributions for lower photon energies are too small to be displayed on this scale, they have been magnified 100 times and are drawn in dashed lines. (Scale to the right of Fig. 2.) The plot of Fig. 2(b) shows the energy of the initial states as we have discussed in Sec. II. We notice that there are two distinct groups of electrons. The initial states of the distributions drawn in solid lines all lie below the top of the valence band ($E-h\nu-E_v<0$). The dashed curves extend to higher energies: $E-h\nu-E_F$

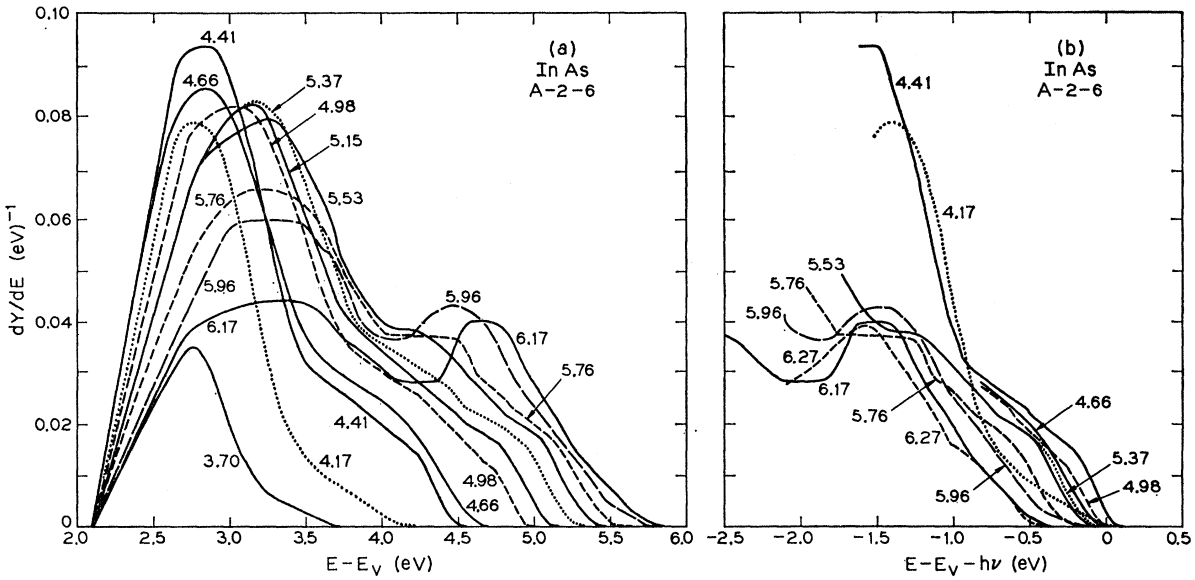

FIG. 5. Energy distributions of photoelectrons from InAs (yield curve A-2-6). (a) Energy of the emitted electrons with respect to the top of the valence band E_v. (b) Energy of the initial states with respect to E_v. The numbers are equal to the photon energies.

$\leqq +0.5$ eV. Note also that the high-energy end of the dashed distributions is as abrupt as the experimental resolution and corresponds to exactly the same initial states for all $h\nu$. Considering that the band gap of InAs at room temperature is $E_g=0.35$ eV, it is reasonable to conclude that the high-energy group of Fig. 2 is due to electrons excited from levels close to the Fermi level and that the latter lies above the bottom of the conduction band at the surface. Such electrons excited from the conduction band have also been observed in the distributions shown in solid lines but cannot be seen on this scale. In the logarithmic plot of the yields, Fig. 1(b), we have marked as a dotted line the yields of which the energy distributions show that they result from excitation of conduction band electrons alone (like the distribution for $h\nu=3.70$ eV on Fig. 2), with a dashed line those which have a significant contribution from conduction and valence electrons (like $h\nu=4.12$, 4.18, and 4.23 eV on Fig. 2), and with a solid line whenever the contribution of conduction electrons, even if observable, is smaller than 1% of the total yield. Curve A-2-1 obtained after deposition of 5.10^{13} cm^{-2} cesium ions shows that the surface is already degenerate n type with $\theta=0.065$ monolayer. We have pointed out in Sec. II that integration of the Poisson equation warrants a band bending of less than 0.05 eV at distances larger than 15 Å from the surfaces. We recall that the electrons escape from a depth of 25 Å at $h\nu=6.17$ eV and more for lower energies in silicon[3] and conclude that no matter how deep the Fermi level lies in the conduction band at the surface, the high-energy end of all distributions due to excitation from the valence band is representative of the position of the bands in the bulk. [The discrepancy between the initial energies of conduction electrons ($E-E_v=0.5$ eV) and the band gap ($E_g=0.35$ eV) can be accounted for by the energy resolution of the experiment and by Ref. 22].

In Fig. 3 we show energy distributions from the clean surface (A-2-0) and after coverage with 5.10^{13} cm^{-2} cesium (surface A-2-1). The distribution for $h\nu=4.41$ eV, surface A-2-1 (dashed line) has been enlarged 100 times; the same analysis as we have done in Fig. 2 shows that those electrons again originate from the neighborhood of the Fermi level which lies inside the conduction band at the surface. Now compare the distributions $h\nu=5.53$ and 6.18 eV from the surface A-2-1 with those from the clean surface A-2-0. The latter are shifted towards higher energies by approximately the amount of the band gap ($E_g=0.35$ eV). Similar distributions were measured at $h\nu=5.76$, 5.96, and 6.27 eV (not shown): they all show the same shift. When the distributions for $h\nu\geq 5.53$ eV from the clean surface are plotted versus $E-h\nu-E_v$ they show the same relative positions as those due to valence electrons in Fig. 2b. We conclude that they result from excitation of valence electrons and that their shift on the energy scale Fig. 3 represents a corresponding shift of the bands with respect to the Fermi level: The clean cleaved 110 surface of InAs is p type; the Fermi level coincides approximately with the top of the valence band at the

[22] The value $E-E_v-h\nu=0$ is placed at the high-energy limit of the distribution for $h\nu=4.41$ eV in Fig. 5(b). It is probable that the E_v so determined is approximately 0.1 eV too low. The $\Gamma_{15v}^{3/2}-\Gamma_{15c}$ splitting is 4.30 eV according to the yield spectra. The high-energy limit for $h\nu=4.41$ may be already lower than the one for $h\nu=4.30$. Unfortunately the lack of a sufficiently intense mercury arc line prevented measurement of dY/dE for $h\nu=4.30$ eV. We also note that our discussion of the lack of influence of the band bending should place the Fermi level at $E_g=0.35$ eV above E_v in Fig. 2. The agreement would be better if E_v were displaced to higher energies. The same applies to the agreement between the initial states at $h\nu=5.53$ to 6.18 eV for the clean surface and those shown in Fig. 5(b).

clean surface. This explains why no evidence of conduction-band electrons was found for the clean surface either in yield [Fig. 1(b)] or in energy distributions. Surface states in the energy gap, if they exist, are essentially empty and do not contribute to the photoelectric yield from the clean surface. The work function of the clean (110) surface of InAs is[7] $\varphi=4.90$ eV: with the Fermi level at the top of the valence band, we find a value for the electron affinity $\chi=\varphi-E_g=4.55\pm0.05$ eV which is different from that previously published.[7]

V. INTERBAND TRANSITIONS

In this section we analyze the yield spectra and energy distributions obtained after the surface barrier has been lowered by deposition of various amounts of cesium. We shall use the criteria outlined in Sec. III to extract information about the optical properties and band structure of InAs. We recall that the n-type doping of the bulk and the degenerate n-type surface allow us to consider the bands as flat within the energy resolution of the retarding field analyzer over most of the volume in which the light is absorbed ($l>100$ Å for all $h\nu$)[23] and from which the electrons escape without appreciable energy losses (≈ 25 Å) for $E-E_F\approx 5$ eV and 150 Å for low $E-E_F$ in Si).[4]

First, we discuss the main features as they appear in the data taken with the lowest work function (A-2-7, $\varphi=1.54$ eV). At low photon energies we observe a smooth rise in yield, until $h\nu=4.17$ eV; Fig. 4 shows that it is mainly due to electrons excited to levels less than 3.25 eV above the top of the valence band. According to the computations by Cohen and Bergstresser,[24] the lowest conduction band extends to energies approximately 3.25 eV above the top of the valence band; it seems reasonable to interpret the low-energy peak of electrons displayed in Fig. 4 in terms of transitions into this lower band. It is possible that this band extends to somewhat higher energies than shown in Fig. 4 and that the sharp decline at the high-energy end of this peak is brought about by energy losses through scattering[18] as we have discussed in Sec. III. This low-energy group still makes a significant contribution to the photoelectric yield at higher photon energies; in fact Fig. 4 shows clearly that its weakening is mainly responsible for the decreasing yield A-2-7 at $h\nu>4.66$ eV. In order to correlate structure in the yield spectrum for $h\nu>4$ eV with energy distributions where $E-E_v>3$ eV, we turn to the yield A-2-6 ($\varphi=2.05$ eV) where low-energy electrons are much less important (see Fig. 5).

Cohen and Phillips[13] have interpreted the peak in the yield spectra (See Fig. 1) at $h\nu=4.36$ eV in terms of a cluster of critical points near the center of the Brillouin zone (Γ). This interpretation is confirmed by the energy distributions: A comparison of the high-energy limits for the distributions $h\nu=4.17$ and 4.41 eV in Fig. 5 shows a sudden accumulation of electrons originating from near the top of the valence band[22] at $h\nu\geq 4.41$ eV (Fig. 5b).

The high-energy limits of the distributions in Fig. 5 are interesting in two respects.

First, we note that the energy distributions for $4.41\text{ eV}\leq h\nu\leq 5.53$ fall off quite abruptly at their high-energy limit. In fact, the distributions fall to zero in an energy range not larger than the resolution of the analyzer ($\Delta E=0.15$ eV). The high-energy end of these distributions is most probably vertical. Such a shape for energy distributions has been predicted theoretically for direct transitions[15] but has not been observed before.

Secondly, the marked change in shape of the upper limit between distributions for $h\nu\leq 4.17$ eV and those for $h\nu\geq 4.41$ eV [Fig. 5(a)] as well as the steady decrease of the abrupt high-energy limit in Fig. 5(b) as $h\nu$ increases above 4.41 eV are clearly incompatible with the shapes of the distributions one expects from a predominance of indirect transitions according to our discussion in Sec. III, Eq. (3).

We now turn our attention to the peak arising near $E-E_v=4.6$ eV in Fig. 5(a) and $E-E_v-h\nu=-1.5$ eV in Fig. 5(b). Its maximum amplitude is reached at $h\nu=5.9$ eV at which photon energy the peak is quite broad, extending from $E-E_v-h\nu=-1.65$ to -1.3 eV. At higher photon energies ($h\nu=6.17$ and 6.27 eV) the initial states [Fig. 5(b)] shift to lower values ($E-E_v-h\nu=-1.6$ eV). Reflectivity data and band-structure computations[24] predict a critical point at the (111) boundary of the Brillouin zone at these photon energies ($L_{3v}-L_{3c}$ transition). The spin-orbit splitting in the valence band at L_{3v} is $\Delta=0.28$ eV.[24] If we interpret our peak in terms of the $L_{3v}-L_{3c}$ transition we are led to conclude that the L_{3v} point in InAs lies between 1.3 and 1.6 eV below the top of the valence band. The shift in peaks evident in Fig. 5(b) then suggests that the majority of electrons are excited from the upper band for $h\nu\leq 5.96$ eV and that the emphasis shifts to the lower band at $h\nu=6.17$ and 6.27 eV. An alternate interpretation of this peak in terms of energy losses of the excited electrons on their way to the surface is ruled out because such a mechanism should depend only on the final energy ($E-E_v$) of the electrons and not on $h\nu$: the position of the peak clearly changes with photon energy in Fig. 5(a). Notice also that the position and the shape of the peak change with $h\nu$ in both plots Figs. 5(a) and 5(b): We have seen in Sec. III that this is an indication of direct transitions.

The energy distributions Figs. 4 and 5 show a broad peak at energies $2.9\leq 3.8$ eV. The distributions for $h\nu\leq 4.66$ eV show no evidence of this peak but at $h\nu=4.98$ the latter is strongly developed. The threshold photon energy for the appearance of this peak thus lies between 4.66 and 4.98 eV. The yield spectra A-2-6 and B-1-2 in Fig. 1 show a peak at these photon energies

[23] G. Harbeke, *Festkörperprobleme* (Friedr. Vieweg und Sohn, Braunschweig, Germany, 1964), Vol. 3, p. 13.
[24] M. L. Cohen and T. K. Bergstresser, Phys. Rev. **141**, 789 (1966).

with threshold at $h\nu = 4.75 \pm 0.05$ eV. According to Figs. 4 and 5(a) the amplitude of this peak increases somewhat up to $h\nu$-5.53 eV and decreases at still higher photon energies. We should like to point out that the position of this peak again changes with $h\nu$ in a manner characteristic of direct transitions (see Sec. III). We cannot suggest an interpretation of this transition in terms of a critical point. Its final states lie between 2.9 and 3.8 eV above the top of the valence E_v, the highest and lowest initial states for this transition lie 1.25 and 3.0 eV below E_v. A similar transition was observed previously with InP.[8]

The reflectivity of InAs displays a strong peak at $h\nu = 4.83$ eV.[19] With III-V compounds this peak is thought to stem from a critical point $X_{5v} - X_{1c}$ at the (100) boundary of the Brillouin zone and usually coincides (within 0.2 eV) with a dip in the yield spectra. This dip is considered proof of the correctness of the interpretation as an X-point transition since the electrons are excited to a low-lying level which prevents escape.[10] Cohen and Phillips[13] attribute the dip which appears in the yield curves at $h\nu < 4.5$ eV to this transition. It may seem presumptuous, after having ascribed the peak at 4.4 eV to the Γ transition, to interpret the end of this peak as a significant dip due to another transition, but the following arguments based on the energy distributions provide a justification for it. We have noted at the beginning of this section that the yield spectrum A-2-7 Fig. 1 is dominated by low-energy electrons while the spectra A-2-6 and A-2-5 are not. The fact that the dip does not depend on the emitted electrons suggests that it is due to non emitting optical transitions. Further, we notice that the high-energy limit of the distributions present an abrupt increase in dY/dE as $h\nu$ changes from $h\nu = 4.17$ to 4.41 eV (Fig. 5) but we see little change as $h\nu$ is further increased. This is an experimental illustration of the fact that the density of transitions does not decrease above a minimum ($\Gamma_{15v} - \Gamma_{1c}$) or an M_1 saddle point[25]: The yield spectra are not necessarily expected to dip after the sharp rise at $h\nu = 4.35$ eV. Finally we note that the behavior of InAs is analogous to that of Si and Ge and III-V compounds[8,11,13,21] which all display a dip in yield spectra correlated with a peak in reflectivity, a behavior which was interpreted in terms of an $X_{5v} - X_{1c}$ transition.

The weak dip the yield spectra associated with the $X_{5v} - X_{1c}$ transition shows that the latter makes a rather small contribution to the peak[19] in ϵ_2 at these photon energies. Kane has come to a similar conclusion in the case of silicon[20] through a theoretical analysis. The yield spectrum A-2-7 suggests that the main contribution to this peak is made by transitions to the whole lower conduction band (Fig. 4).

We do not discuss at this point the find structure which is observed reproducibly in the energy distributions Figs. 4 and 5 for lack of a more detailed knowledge of the band structure of InAs. Such an interpretation would require an analysis similar to that performed by Kane for silicon.[20]

VI. CONCLUSIONS

The energy distributions of photoelectrically emitted electrons have provided information about surface properties and optical transitions in InAs.

The clean cleaved (110) surface of InAs is p type on a moderately n-type bulk: the Fermi level coincides with the top of the valence band at the surface. Deposition of 1/20 monolayer of cesium results in a degenerate n-type surface; this result points to a low density of surface states in the energy gap. Measured energy distributions allow to identify two distinct groups of electrons originating in the conduction band close to the surface and in the valence band. Changes in band bending are observed directly as shifts in the position of energy distributions. The experiments show that photoemission from surface states with a density of 10^{13} cm^{-2} could be observed if the optical transitions are allowed. The electron affinity and work function of the cleaved (110) surface of InAs are $\chi = 4.55 \pm 0.05$ eV and $\varphi = 4.90 \pm 0.05$ eV, respectively.

As far as the optical properties of InAs are concerned, the energy distributions have yielded confirmation of the $\Gamma_{15v} - \Gamma_{15c}$ splitting at $h\nu = 4.30$ eV with proof of a strong predominance of direct transitions, confirmation of the L_{3v}-L_{3c} transition around $h\nu = 6.0$ eV with a corrected position of L_{3v}, support to the X_{5v}-X_{1c} transition at 4.50 eV, a previously unknown transition with threshold at $h\nu = 4.80$ eV and a broad group of transitions to the lower conduction band with its maximum approximately at $h\nu = 4.5$ eV.

The energy distributions also contain reproducible fine structure which we have not interpreted for lack of detailed knowledge of the band structure. Whenever information was obtained about the optical excitation mechanism, it pointed to direct transitions.

ACKNOWLEDGMENTS

The authors wish to thank E. O. Kane for helpful discussions and prepublications access to his work, and A. A. Studna, B. Hennion, and W. Emslie for skillful technical cooperation.

[25] G. H. Wannier, *Elements of Solid State Theory* (Cambridge University Press, London, 1959), p. 70.